Xu et al. Cell Communication and Signaling (2024) 22:550
https://doi.org/10.1186/s12964-024-01926-x

Cell Communication and Signaling

METHODOLOGY Open Access

USP11 promotes lipogenesis and tumorigenesis by regulating SREBF1 stability in hepatocellular carcinoma

Yongkang Xu[1], Jiayu Zeng[2], Kan Liu[1], Dan Li[3], Shenglan Huang[1], Shumin Fu[1], Mao Ye[1], Si Tao[1] and Jianbing Wu[1*]

Abstract

Background The relationship between hepatocellular carcinoma (HCC) metastasis and cancer metabolism reprogramming is becoming increasingly evident. Ubiquitin-specific protease 11 (USP11), a member of the deubiquitinating enzyme family, has been linked to various cancer-related processes. While USP11 is known to promote HCC metastasis and proliferation, the precise mechanisms, especially those related to cancer metabolism, remain unclear.

Methods Through mass spectrometry, co-immunoprecipitation, immunofluorescence, and ubiquitination assays, we identified USP11 as the key deubiquitinase for SREBF1.Lipogenesis was evaluated using Oil Red O and Nile Red staining, along with the detection of triglycerides and cholesterol. To assess HCC cell proliferation, migration, and invasion in vitro, Transwell assays, EDU, colony formation, and CCK-8 were conducted. Xenograft models in nude mice were developed to verify the role of the USP11/SREBF1 axis in lipogenesis and tumor growth in vivo.

Results USP11 directly interacts with SREBF1, and its silencing leads to the disruption of SREBF1 stabilization through K48-linked deubiquitination and degradation. Importantly, the truncated mutant USP11 (503–938 aa) interacts with the truncated mutant SREBF1 (569–1147aa), with K1151 playing a crucial role in this interaction. Higher levels of USP11 enhance lipogenesis, proliferation, and metastasis in HCC cells. Importantly, the knockdown of SREBF1 weakened the effects of USP11 in enhancing lipogenesis and tumorigenesis. Futhermore, the elevated expression of USP11 and SREBF1 in HCC tissue serves as an indicator of poor prognosis in HCC patients.

Conclusions In summary, our study reveals that USP11 promotes HCC proliferation and metastasis through SREBF1-induced lipogenesis. These findings provide a foundation for novel therapies targeting lipid metabolism in HCC.

Keywords Hepatocellular carcinoma, USP11, SREBF1, Lipogenesis, Tumorigenesis

*Correspondence:
Jianbing Wu
hhgwjb@163.com
[1]Department of Oncology, The Second Affiliated Hospital, Jiangxi Medcical College, Nanchang University, Nanchang, Jiangxi Province 330006, China
[2]Department of Pediatric Surgery, Jiangxi Provincial Children's Medical Center, Jiangxi Maternal and Child Health Hospital, Nanchang, Jiangxi Province, China
[3]Department of Gastroenterology, The Second Affiliated Hospital, Jiangxi Medcical College, Nanchang University, Nanchang, Jiangxi Province, China

Introduction

Hepatocellular carcinoma (HCC) is a highly heterogeneous tumor within the digestive system, with increasing global incidence and mortality rates [1]. Tumor heterogeneity in HCC results in diverse signaling pathways and phenotypic variations, posing challenges for personalized cancer therapies [2].HCC is recognized as a typical metabolism-related tumor, marked by abnormalities in amino acid, lipid, and carbohydrate metabolism [3]. The liver, a crucial organ for human lipid metabolism, undergoes significant lipid compositional changes during the malignant progression of HCC. This suggests targeting abnormal lipid metabolism may be a promising therapeutic strategy for treating HCC. However, the molecular mechanisms regulating lipid metabolism in HCC remain poorly understood.

Sterol regulatory element-binding transcription factor 1 (SREBF1) is a critical regulator of lipid metabolism, primarily involved in biosynthesizing and metabolizing endogenous cholesterol, fatty acids, phospholipids, and triglycerides [4]. It significantly impacts the lipid metabolism processes of cancer cells by transcriptionally regulating the expression of a series of key metabolic enzymes. Numerous studies have reported that SREBF1, acting as a transcription factor, promotes the mRNA expression of metabolic enzymes such as ACLY [5], FASN [6], ACACA [7], and SCD1 [8].Studies have identified aberrant SREBF1 expression in cancers like colorectal cancer, HCC, prostate cancer, and endometrial cancer, closely linked to poor patient prognosis, underscoring its pivotal role in tumor progression [8–11]. Furthermore, Liu et al. demonstrated that Treg cells promote the SREBF1-dependent metabolic adaptation of tumor-supporting macrophages by suppressing interferon-γ production from CD8+ T cells [12]. However, the upstream role of SREBF1 in cancer biology remains undefined. Therefore, a thorough exploration of the specific mechanisms of SREBF1 in HCC development may provide new insights for the diagnosis and treatment of this disease.

The ubiquitin-proteasome pathway is pivotal for intracellular protein degradation, essential for regulating cell cycle dynamics, division signaling pathways, protein quality maintenance, and clearing aberrant proteins due to misfolding or damage [13, 14].Ubiquitination and deubiquitination are critical post-translational modifications of metabolic enzymes, intricately regulating their degradation, subcellular localization, and activation, profoundly influencing metabolic reprogramming in tumors [15, 16].Recent research highlights the role of TRIM21 in renal cell carcinoma (RCC), where it curtails lipid accumulation by regulating the ubiquitination and subsequent degradation of SREBF1 [17]. Dysregulation of ubiquitination and deubiquitination is closely associated with altered cellular lipid metabolism, promoting the development and progression of various cancers, including HCC [18, 19]. Recent studies across multiple cancers highlight deubiquitinating enzymes (DUBs) due to their potential in stabilizing oncogenic proteins [20]. For example, USP22 significantly enhances lipid accumulation in HCC cells by bolstering the deubiquitination stability of PPARγ [21].This study utilized comprehensive approaches such as Co-IP, LC-MS, and ubiquitination modification omics, identifying USP11 as a potent DUB within the expansive cysteine protease DUB subfamily.USP11 emerges as an effective regulator of SREBF1 through targeted deubiquitination. Despite previous characterization of USP11 as an oncogenic driver in HCC, its role in modulating cancer lipid metabolism remains unexplored. Therefore, our investigation delves deeper into understanding how USP11 impacts HCC progression via its interaction with SREBF1.

Our study reveals a novel pathway wherein USP11 promotes lipid metabolism in HCC cells. USP11 is identified as a novel deubiquitinase of SREBF1, mediating its ubiquitination degradation in a k48-linked manner. Reduced ubiquitination of SREBF1 leads to increased transcriptional expression of downstream lipid metabolism-related genes, thereby further promoting lipid metabolism in HCC cells. Furthermore, the expression of SREBF1 is positively correlated with the expression of USP11 in clinical tissue samples.

Materials and methods

Cell cultures

The human normal liver cell line LO2 and HCC cell lines Huh7, MHCC97H, HCC-LM3, and HepG2 were obtained from the Cell Bank of the Chinese Academy of Sciences. The cell lines were cultured in high-glucose DMEM supplemented with 10% fetal bovine serum in a 37 °C incubator with 5% CO2.

Western blot analysis and antibodies

Cells were lysed using RIPA buffer (Solarbio Biotechnology, China) supplemented with protease inhibitors and phosphatase inhibitors (Solarbio Biotechnology, China). Protein concentrations were detected using a BCA protein assay reagent (Beyotime Biotechnology, China). Cellular extracts were separated by SDS-PAGE, transferred to PVDF membranes (Millipore, Billerica, USA), and then incubated with the corresponding primary antibodies. The specific antibody signals were analyzed using an enhanced chemiluminescent substrate kit (Solarbio Biotechnology, China). Relative protein abundance was quantified by gray-scale scanning using Image Lab analysis software (version 4.0, Bio-Rad) and ImageJ (ImageJ 1.53). Antibodies used in this study were shown in Table S1.

Co-immunoprecipitation (Co-IP) and LC-MS/MS analysis

In the Co-IP experiment, cells were lysed using Western and IP cell lysis buffer (Beyotime Biotechnology, China). The cell lysates were incubated overnight at 4 °C with specific primary antibodies, followed by incubation with protein A/G sepharose beads (Santa Cruz, USA). The coprecipitated proteins were then detected using immunoblotting with the specified antibodies.

For anti-SREBF1 immunoprecipitation from HCCLM3 cell lysates, the same Co-IP method was employed. Immunoprecipitates were mixed with electrophoresis sample buffer and subjected to SDS-PAGE. SDS-PAGE gels were stained with Coomassie blue staining for 3 h and washed with eluent overnight. The gels were analyzed by liquid chromatography-tandem mass spectrometry (LC-MS/MS) (Jikai Gene (Shanghai) Life Technology Co., Ltd.). The results for the LC-MS/MS are provided in Table S2.

Immunofluorescence staining

Cells were seeded into 6-well plates and cultured for 12 h. The cells were then fixed with 4% paraformaldehyde for 30 min and permeabilized with 0.5% Triton-X for 10 min. Blocking was performed using 5% BSA at room temperature for 60 min. Primary antibodies were applied and incubated with the cells overnight at 4 °C. Subsequently, the cells were washed three times with cold PBS, followed by incubation with secondary antibodies in the dark for 1 h. Finally, DAPI-containing mounting medium (P0131, Beyotime) was used to stain the nuclei, and fluorescence images were acquired using a confocal microscope (Leica TCS SP8).

Plasmids and siRNA/shRNAs transfection and lentiviral transduction

HA-tagged USP11 expression vectors (including 1-963aa, 1-938aa, 1-284aa, 503-963aa, and 285-963aa), siRNA sequences targeting USP11, SREBF1 mutants (K617R, K705R, K954R, K1100R, K1151R) and mutated ubiquitin vectors (His-Ub K6, His-Ub K48, and His-Ub K63), were custom synthesized by Hanbio Biotechnology Co., Ltd. (Shanghai, China). Similarly, FLAG-tagged SREBF1 expression vectors (1-1147aa, 1-568aa, 488-1147aa) and siRNA/shRNA sequences targeting SREBF1 were synthesized by GENERAL Biotechnology Co., Ltd. (Anhui, China). Lipofectamine 3000 transfection reagent (Invitrogen, USA) was used for introducing these plasmids into cells following the manufacturer's protocol. The specific sequences of the siRNA/shRNAs are provided in Table S1.

To establish cell lines with stable downregulation of USP11 and upregulation of SREBF1, lentiviral vectors expressing USP11, SREBF1, and puromycin resistance genes were employed. HCC cells were transfected with lentiviral vectors carrying USP11 (MOI=10) and SREBF1 (MOI=15). After 48 h of infection, the medium was replaced with fresh medium containing puromycin to select stably infected clones.

Quantitative real-time PCR

Total RNA was extracted from HCC cells and tissue samples using TRIzol reagent (Invitrogen, Carlsbad, CA, USA). RNA was then reversetranscribed into complementary DNA (cDNA) with the PrimeScript™ RT reagent kit, which includes a gDNA Eraser (RR047A, TaKaRa, China). Quantitative PCR was carried out using TB Green® Premix Ex Taq™ II (RR820A, TaKaRa, China) on a CFX96 real-time PCR system. The amplification conditions were set at 94 °C for 30 s, followed by 40 cycles of 94 °C for 4 s, 58 °C for 15 s, and 72 °C for 15 s. Relative mRNA levels in HCC cells were quantified using the $2-\Delta\Delta Ct$ method. Primer sequences are detailed in Table S3.

In vivo ubiquitination assays

For in vivo ubiquitination analysis, HCC or HEK-293T cells were transfected with specific shRNAs or plasmids. After transfection, cells were treated with 15 μM MG132 for 6-8 h to inhibit proteasomal degradation. Subsequently, cells were lysed using the Co-IP assay protocol, followed by immunoprecipitation and Western blot analysis of the samples.

Patients and specimens

A total of 78 pairs of primary hepatocellular carcinoma (HCC) specimens were collected from patients who had not received radiotherapy or chemotherapy before their surgery. Clinical data for these patients were retrieved from the medical records at the Second Affiliated Hospital of Nanchang University. This research adhered to the Declaration of Helsinki and received approval from the Ethics Committee of the Second Affiliated Hospital of Nanchang University.

Bioinformatics analysis

The RNA sequencing data from various tumors were sourced from the TIMER2.0 (Tumor IMmune Estimation Resource 2.0) database (http://timer.comp-genomics.org/). We downloaded and organized the RNAseq data processed by the STAR pipeline from the TCGA-LIHC project via the TCGA database (https://portal.gdc.cancer.gov), extracting data in FPKM format along with corresponding clinical data.

Immunohistochemistry (IHC) staining

Fresh tissue samples were collected immediately after resection and fixed in 10% formalin. The samples were then embedded in paraffin, sectioned into 3–4 μm thick

slices, mounted on glass slides, and baked at 60 °C for 2 h. All tissue sections were deparaffinized with xylene, rehydrated with ethanol, and subjected to antigen retrieval with EDTA. Endogenous enzyme activity was blocked with 0.3% hydrogen peroxide. The sections were incubated overnight at 4 °C with the primary antibody of interest (1:200 dilution). Subsequently, the sections were incubated at room temperature for 30 min with a secondary antibody (polyperoxidase-anti-rabbit IgG) conjugated with horseradish peroxidase, then stained with diaminobenzidine (DAB) and counterstained with hematoxylin. The staining intensity was assessed using the ImageJ.

Nile red staining

HCC cells were cultured in a 96-well plate, washed with PBS, fixed with 4% paraformaldehyde, and then stained with Nile Red dye (Beyotime, China, Cat. No. C2053S). Images were captured using a fluorescence microscope. Cellular fluorescence intensity was analyzed and quantified using ImageJ software, with the average fluorescence intensity normalized to the cell number.

Oil red O staining

HCC cells were seeded into 6-well plates and cultured overnight. The cells were stained using a cell-specific Oil Red O solution (Solarbio, Beijing, China, Cat. No. G1262), following the manufacturer's instructions. The average cellular staining intensity was analyzed and quantified using ImageJ software and normalized to the cell number. Additionally, frozen sections from mouse xenograft tumors were stained with Oil Red O, first fixed with formalin for 30 min. Subsequently, they were stained with the Modified Oil Red O Stain Kit (Solarbio, Beijing, China, Cat. No. G1261) for 15 min. After staining, the sections were washed with water for 2 min and rinsed with 60% isopropanol for 1 min to remove excess dye. The nuclei were then stained with hematoxylin for 1 min.

Triglyceride and cholesterol detection

Cellular and tumor triglyceride (TG) and cholesterol (TC) levels were quantified using tissue TG and TC content assay kits from Applygen Technologies Inc. (Beijing, China, Cat. No. E1013-50,E1015-50), following the manufacturer's instructions. Protein concentrations were measured using a BCA Protein Assay Kit from Beyotime Biotechnology (Shanghai, China). The TG and TC levels were then normalized to the protein concentration.

Cell proliferation and 5-Ethynyl-2′-deoxyuridine (EdU) assay

For assessing cell proliferation, HCC cells were plated at a density of 3000 cells/well in a 96-well format, followed by the addition of 10 μL CCK-8 reagent. The plates were then incubated at 37 °C for 2.5 h, after which the absorbance at 450 nm was determined to quantify cell growth. The cells were incubated with EdU staining solution (Epizyme, CX003,China) for 2 h at 37 °C, followed by fixed with 4% paraformaldehyde for 30 min at room temperature. After fixation, the cells were washed with 3% bovine serum albumin (BSA) and permeabilized with 0.1% Triton X-100. EdU staining reagents were then applied following the manufacturer's guidelines. Then the cells were stained with 100 μL of 1× Hoechst 33,342 solution for 30 min. Positive EdU staining was examined under a fluorescence microscope, and the percentage of proliferating cells was quantified using ImageJ software.

Migration and invasion assays, colony formation and flow cytometry analysis

For the migration assay, 200 μL of serum-free medium with $2\times10^{\wedge4}$ HCC cells was placed in the upper chamber of Transwell inserts, and the lower chamber was filled with 700 μL medium containing 20% FBS. After incubation for 24–48 h, the cells were stained with crystal violet.

In the invasion assay, the Transwell membrane was precoated with a 1:8 dilution of Matrigel and left to solidify for 3 h. Then, 200 μL of serum-free medium with $2\times10^{\wedge4}$ cells was added to the upper chamber, and 700 μL of medium with 20% FBS was added to the lower chamber. The cells were incubated for 48–96 h at 37 °C, and invasive cells were stained with crystal violet.

For the colony formation assay, HCC-LM3 cells were seeded at 500 cells/well, and Huh7 and HepG2 cells at 1000 cells/well in six-well plates. Cultures were grown for 10–14 days until colonies exceeded 50 cells, and then stained with methyl violet for 30 min.

To assess cell apoptosis, we used the FITC-annexin V and PI apoptosis detection kits (UElandy, Suzhou, China) according to the manufacturer's protocol. Transfected cells grown in 6-well plates were harvested with EDTA-free trypsin (Solarbio Biotechnology, Beijing, China) and washed three times with PBS. The cells were then resuspended in 100 μL of mixed buffer to achieve a concentration of $1\times10^{\wedge5}$ cells/ml. Next, 5 μL of FITC-annexin V and 5 μL of PI were added. After a 15-minute incubation in the dark at 4 °C, 400 μL of mixed buffer was added. The percentage of apoptotic cells, including early and late stages, was analyzed using Beckman CytoFLEX.

Xenograft tumorigenicity assay

To establish subcutaneous xenograft models, 3-4week old female BALB/c nude mice were purchased from Hangzhou Ziyuan Biotechnology Co., Ltd. Each mouse was subcutaneously injected with $3\times10^{\wedge6}$ HCC-LM3 cells that stably express shNC, shUSP11, Vector and SREBF1. Tumor growth was recorded every 7 days. Tumor volume was calculated using the formula: Tumor volume (mm^3)

= (length × width^2) / 2. When significant differences in tumor growth between groups were observed, the mice were euthanized, tumors were excised and weighed, and the tumor tissues were sliced for further experiments.

Statistical analysis

All data are expressed as mean±standard deviation from at least three independent experiments. Comparison between two groups was performed using Student's *t*-test, while comparisons among multiple groups were analyzed with one-way ANOVA followed by Tukey's multiple comparison test. The Chi-square test was utilized to evaluate the association between the target genes expression and clinicopathological features. Kaplan–Meier survival curves were assessed using the log-rank test. Pearson correlation analysis was used to assess the correlation. All data analysis was conducted by Prism 9.0 (GraphPad Software, CA, USA) or SPSS 26.0(SPSS Inc., Chicago, IL, USA). Statistical significance was defined as * $p<0.05$, ** $p<0.01$, *** $p<0.001$ and **** $p<0.0001$, ns: no significance.

Results

USP11 interacts with SREBF1

To elucidate the molecular mechanism by which SREBF1 promotes the development and metastasis of HCC, researchers used immunoaffinity purification to extract SREBF1-interacting proteins in HCC-LM3 cells and identified them through LC-MS/MS (Table S2). Among the identified proteins was the deubiquitinating enzyme USP11 (Fig. 1A). Consistent with the mass spectrometry results, Co-IP assays demonstrated interactions between endogenous SREBF1 and USP11 in HCC-LM3, HepG2, and Huh7 cells (Fig. 1B). Importantly, HA-tagged USP11 and Flag-tagged SREBF1 were co-detected when expressed ectopically, indicating their interaction (Fig. 1C). Next, immunofluorescence staining confirmed that they are primarily colocalized in the cytoplasm, with a small portion distributed in the nuclei of HCC-LM3, HepG2, and Huh7 cells (Fig. 1D). To identify the specific interaction regions between USP11 and SREBF1, researchers generated truncated mutant fragments of both proteins and determined their binding sites (Fig. 1E). Transfection experiments in HEK-293T cells showed that deleting amino acids 1-284 in USP11 weakened its binding capacity with SREBF1. This indicates that the crucial binding region for SREBF1 lies between amino acids 503–938 of USP11(Fig. 1F). For SREBF1, deletion of amino acids 1-568 resulted in loss of binding with USP11. These findings highlight the critical binding region with USP11 lying between amino acids 569–1147 of SREBF1(Fig. 1F). Collectively, these data demonstrate that USP11 is a bona fide interacting protein of SREBF1.

USP11 stabilizes SREBF1

To explore the regulatory influence of USP11 on SREBF1, researchers conducted USP11 knockdown experiments in HCC-LM3 and HepG2 cells. The results revealed a notable reduction in SREBF1 protein levels, despite no significant changes in SREBF1 mRNA expression, indicating that USP11 affects SREBF1 post-transcriptionally (Fig. 2A/D). Further investigation showed that the suppression of USP11 led to proteasome-dependent destabilization of the SREBF1 protein, which was effectively counteracted by the application of the proteasome inhibitor MG132, underscoring the role of the proteasome in this process (Fig. 2B-C). To further examine the effect of USP11 on SREBF1 protein stability, CHX was used to block protein synthesis. In USP11 knockdown cells, rapid degradation of SREBF1 was observed, emphasizing the critical role of USP11 in protecting SREBF1 from proteasomal degradation. Moreover, SREBF1 exhibited a significantly longer half-life in Huh7 cells overexpressing USP11(Fig. 2D-G). These results indicate that USP11 tightly controls the stability of the SREBF1 protein.

USP11 deubiquitinates SREBF1

Researchers observed that knocking down USP11 in HCC-LM3 and HepG2 cells increased the endogenous ubiquitination levels of SREBF1(Fig. 3A/B). Conversely, transfecting overexpression of USP11 decreased ubiquitination levels of SREBF1 in Huh7 cells (Fig. 3C). Additionally, in vitro experiments have also demonstrated that HA-USP11 can significantly promote the deubiquitination of Flag-SREBF1(Fig. 3D). To determine which type of SREBF1 ubiquitination is influenced by USP11, researchers co-transfected HA-USP11, Flag-SREBF1, and seven lysine-specific ubiquitin mutants (K6, K48 and K63) into HEK-293T cells. USP11 was found to specifically cleave the K48-linked polyubiquitin chains on the SREBF1 protein (Fig. 3E). Through ubiquitination site prediction, researchers identified 11 potential USP11 target sites on the SREBF1 protein. Based on the previous functional regions, they selected 5 amino acid sites (K617, K705, K954, K1100, K1151) for mutation. Overexpression of USP11 with K617R, K705R, K954R, K1100R resulted in a reduced level of SREBF1 protein ubiquitination. However, overexpression of USP11 with K1151R had little effect on the ubiquitination level of the SREBF1 protein. Thus, lysine-1151 may be an important site for USP11 regulation of SREBF1 deubiquitination (Fig. 3F).

USP11 deficiency inhibits lipogenesis and proliferation of HCC cells in vivo and in vitro

The aforementioned studies demonstrate an interaction between USP11 and the key lipid metabolism regulator SREBF1, with previous research suggesting that USP11 may be associated with cancer metabolism. To further

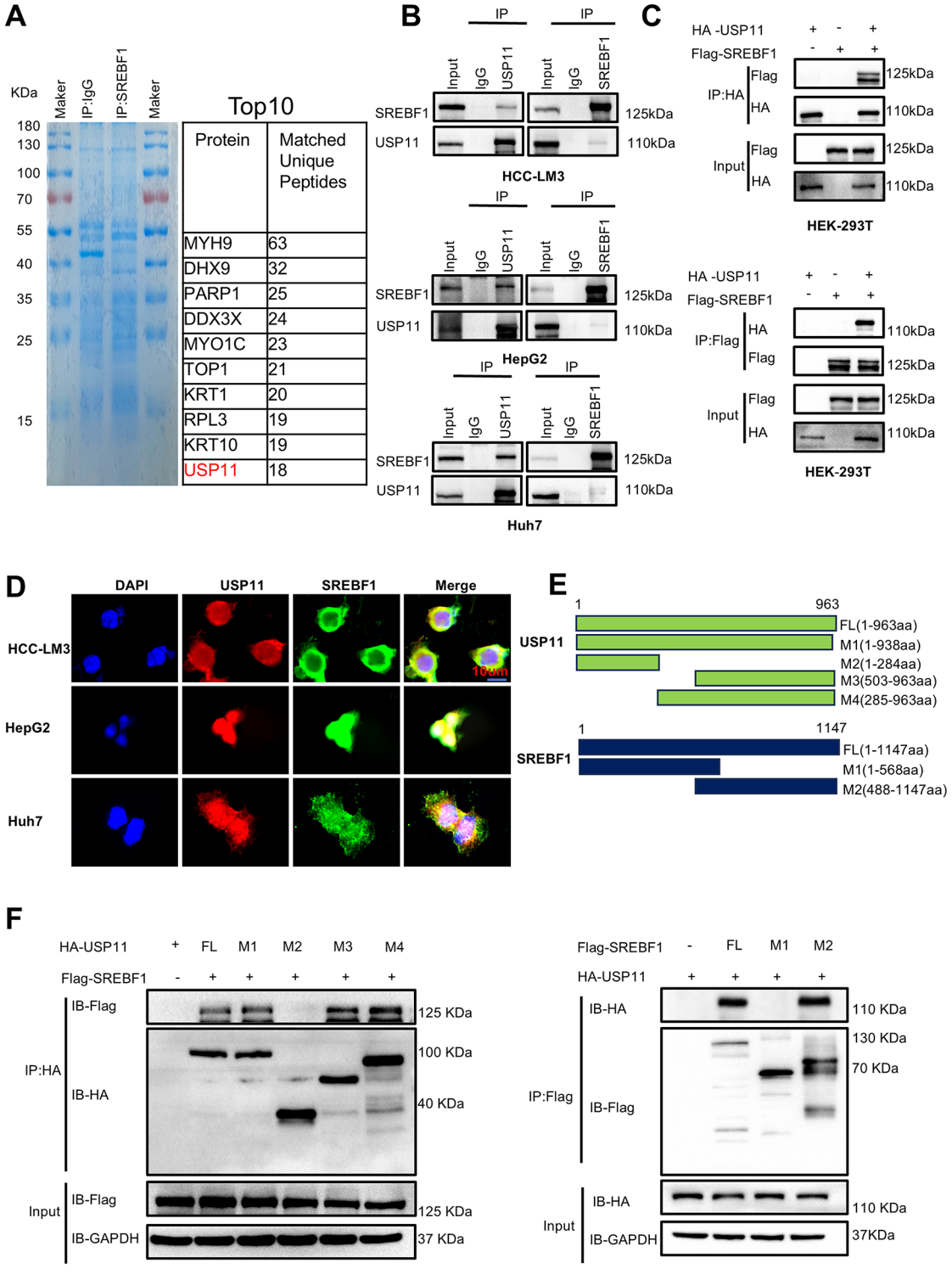

Fig. 1 USP11 interacts with SREBF1. **A**. In HCC-LM3 cells, anti-SREBF1 antibodies were used for immunoprecipitation. The co-immunoprecipitated proteins was stained with Coomassie blue staining and analyzed by mass spectrometry. **B**. Co-IP revealed interactions between endogenous USP11 and SREBF1 in HCC-LM3, HepG2, and Huh7 cells. **C**.HA-USP11 and Flag-SREBF1 were co-transfected into HEK-293T cells. Co-IP was performed to demonstrate interactions between exogenous USP11 and SREBF1. **D**. Confocal microscopy was used to analyze the localization of USP11 (red) and SREBF1 (green) in HCC-LM3, HepG2, and Huh7 cells, with nuclei stained with DAPI (blue). Scale bar: 10 μm. **E**. Diagrammatic presentation of USP11 and SREBF1 protein full length and various deletion mutants. **F**. Co-IP assays were performed using anti-HA or anti-Flag antibodies with HA-USP11 and Flag-SREBF1 or their deletion mutants

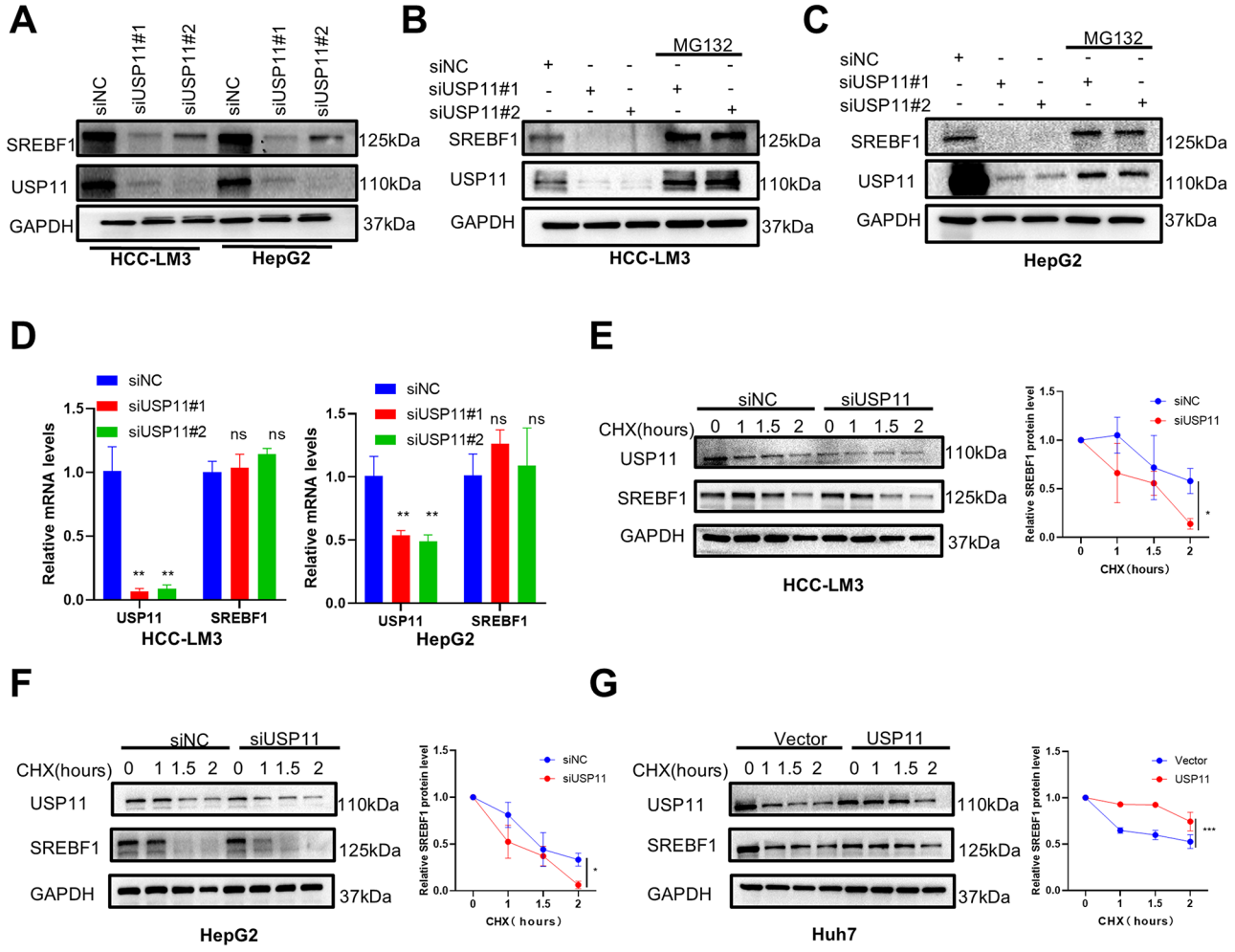

Fig. 2 USP11 regulates SREBF1 stability. **A**. Western blot was used to assess the expression of SREBF1 in HCC-LM3 and HepG2 cells transfected with USP11 siRNA. **B**, **C**. Western blotting showed that the proteasome inhibitor MG132 reversed SREBF1 protein levels in USP11 knockdown HCC-LM3 and HepG2 cells. **D**. The mRNA expression level of SREBF1 in HCC-LM3 and HepG2 cells transfected with USP11 siRNA. **E**, **F**. USP11 was knocked down by siRNA in HCC-LM3 and HepG2 cells, followed by treatment with CHX (40 μM) for the indicated times. USP11 and SREBF1 protein levels were determined by Western blot. **G**. Huh7 cells were transfected with USP11 overexpression plasmid or empty vector, followed by treatment with CHX (40 μM) for the indicated times. USP11 and SREBF1 protein levels were determined by Western blot. *$p < 0.05$; ** $p < 0.01$; *** $p < 0.001$; ns: no significance

clarify the crucial role of USP11 in lipid metabolism, we performed USP11 knockdown or overexpression experiments. Oil Red O staining and Nile red detection methods showed that siRNA knockdown of USP11 reduced lipid synthesis in the HCC-LM3 (Fig. 4A) and HepG2 cells (Fig. S2A), whereas overexpression of USP11 enhanced lipid synthesis (Fig. 4B) in Huh7 cells. Additionally, knockdown of USP11 resulted in decreased levels of triglycerides and cholesterol in the HCC-LM3 (Fig. 4C) and HepG2 cells (Fig. S2B), whereas overexpression of USP11 enhanced lipid synthesis (Fig. 4D) in Huh7 cells. Western blot and RT-qPCR analysis revealed reduced levels of ACLY, FASN, ACACA and SCD1 in USP11-deficient HCC cells (Fig. 4E/G, Fig. S2C-D), which differs from the results observed with USP11 overexpression in Huh7 cells (Fig. 4F/H).

Due to lipid metabolism dysregulation potentially driving malignant progression in HCC, we subsequently assessed the impact of USP11 on the malignancy of HCC cells. Notably, we established the oncogenic role of USP11 through bioinformatics analysis as well as clinical tissue samples and HCC cell lines (Fig. S1). Researchers investigated the biological functions of USP11. Transwell assays indicated that silencing USP11 inhibited the invasion and migration of HCC cells (Fig. 5A, Figure S2E), while overexpressing USP11 promoted these processes (Fig. 5B). EdU and CCK-8 assays were used to assess cell proliferation and viability. The results showed that knocking down USP11 with siRNA significantly reduced cell proliferation and viability (Fig. 5C/E, Fig. S2E-F), whereas overexpressing USP11 enhanced both proliferation and viability (Fig. 5D/E). Cell apoptosis assays

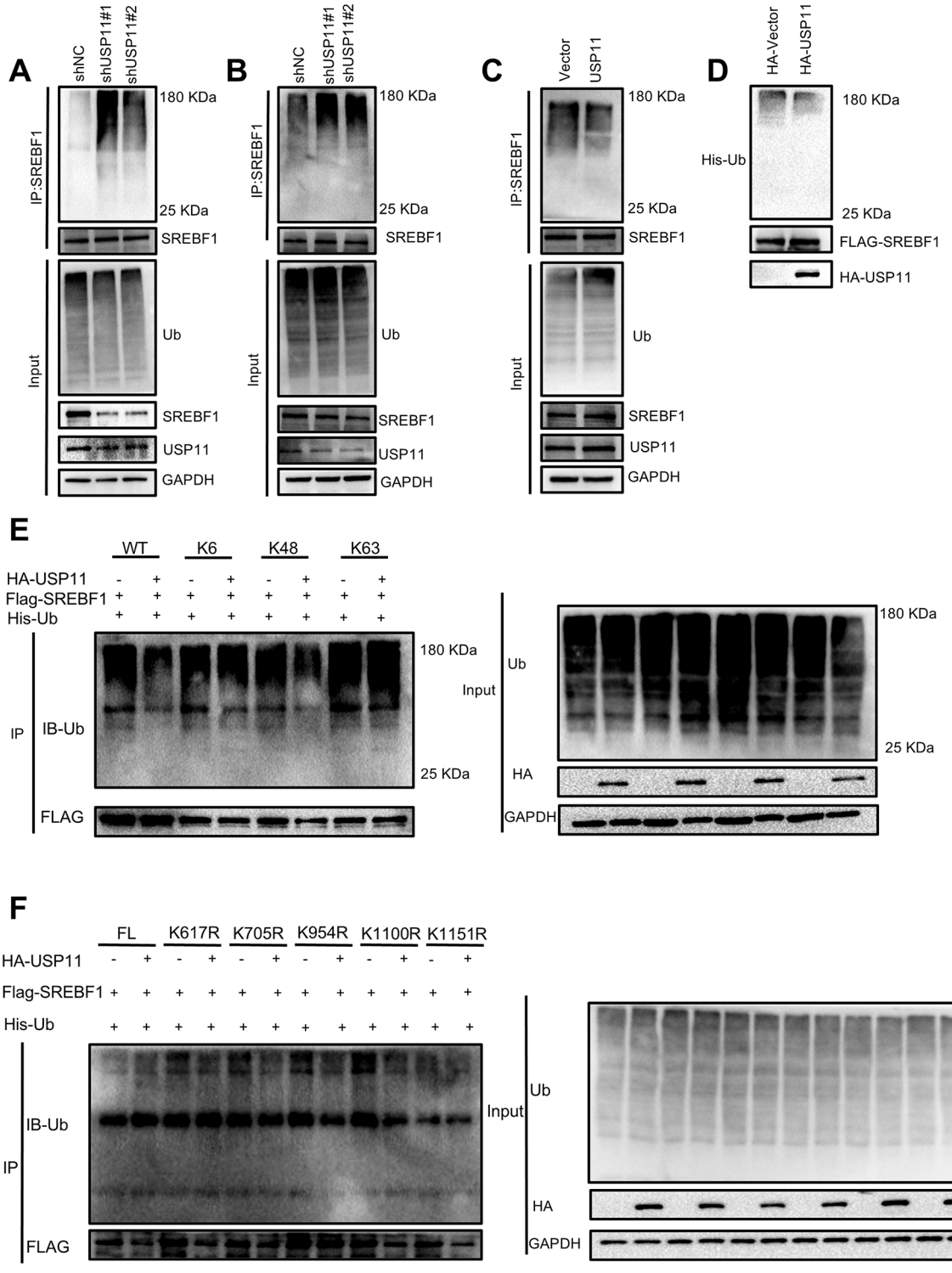

Fig. 3 USP11 deubiquitinates SREBF1. **A**, **B**. HCC-LM3 and HepG2 cells transfected with shNC or shUSP11#1/2 were immunoprecipitated, and SREBF1 ubiquitination was detected by Western blotting. **C**. Huh7 cells overexpressing USP11 and transfected with Vector or USP11 were immunoprecipitated, and SREBF1 ubiquitination was detected by Western blotting. **D**. In vitro deubiquitination assay of ubiquitinated Flag-SREBF1 protein using purified HA-tagged USP11. **E**. HA-USP11, Flag-SREBF1, His-Ub, or Ub mutants (K6R, K48R, K63R) plasmids were co-transfected into HEK-293T cells, which were then treated with 15 μM MG132 for 6-8 h. Co-IP revealed the polyubiquitination of SREBF1 in HEK-293T cells. **F**. Ubiquitination assay of SREBF1 in HEK-293T cells co-transfected with His-Ub, HA-USP11, and FLAG-SREBF1 mutants (K617R, K705R, K954R, K1100R, K1151R) and treated with 15 μM MG132 for 6-8 h

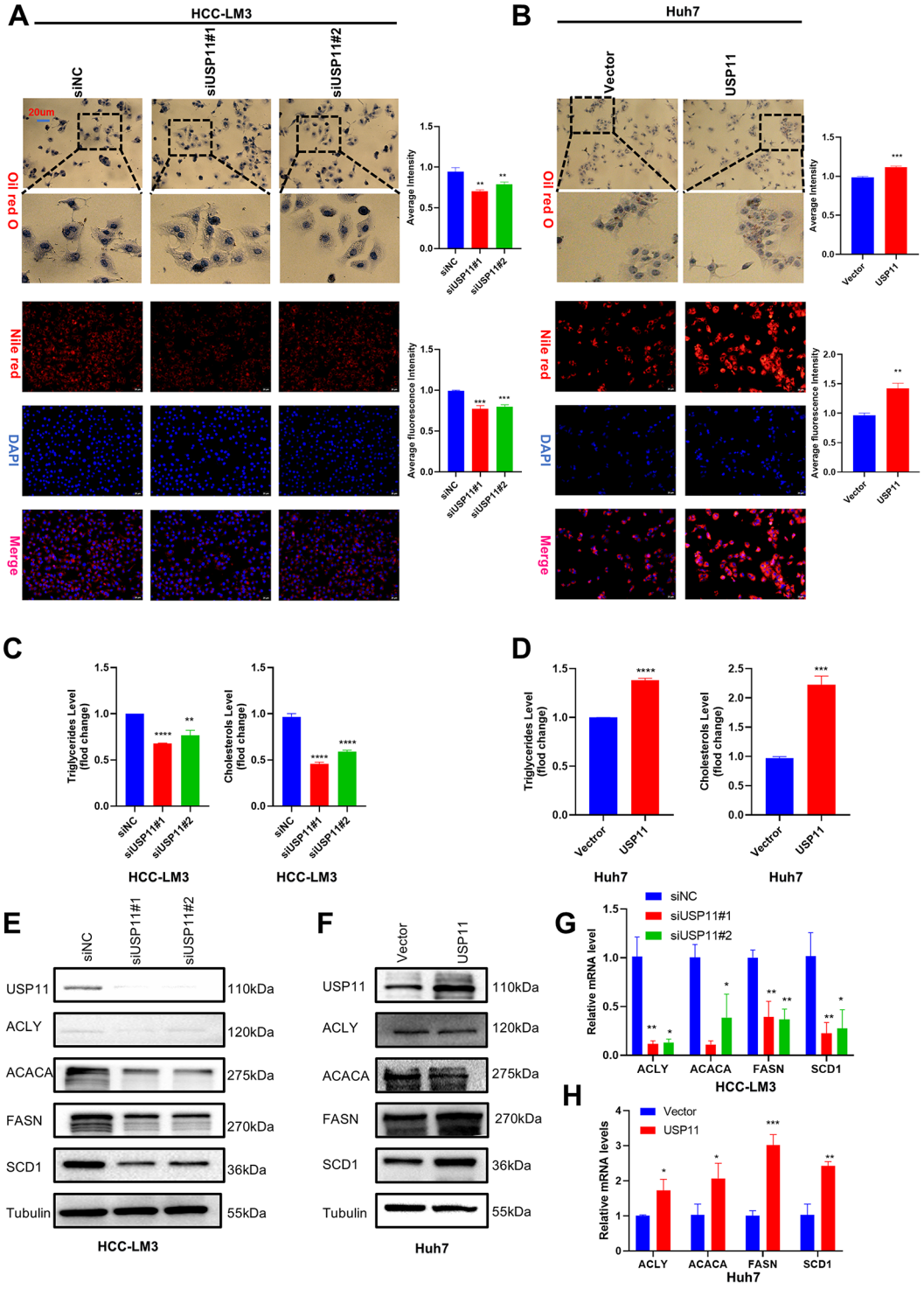

Fig. 4 USP11 deficiency attenuates lipogenesis in HCC cells. **A**. Oil red O staining (Upper) and Nile red staining (Lower) were used to evaluate the formation of lipids in HCC-LM3 cells transfected with control siRNA or USP11 siRNA. Scale bars, 20 μm. **B**. Oil red O staining (Upper) and Nile red staining (Lower) were employed to assess lipid formation in Huh7 cells transfected with Vector or USP11. Scale bars, 20 μm. **C**. Triglycerides (Left panel) and cholesterol (Right panel) in HCC-LM3 cells transfected with control siRNA or USP11 siRNA were quantified using tissue-cell assay kits for triglycerides and total cholesterol. **D**. Triglycerides (Left panel) and cholesterol (Right panel) in Huh7 cells with USP11 overexpression were quantified using tissue-cell assay kits for triglycerides and total cholesterol. **E**. Western blot detection of USP11, ACLY, FASN, ACACA, and SCD1 protein expression in USP11-knockdown HCC-LM3 cells. **F**. Western blot detection of USP11, ACLY, FASN, ACACA, and SCD1 protein expression in Huh7 cells with USP11 overexpression. **G, H**. RT–qPCR were utilized to measure the mRNA levels of ACLY, FASN, ACACA, and SCD1 in HCC-LM3 and Huh7 cells. *$p < 0.05$, **$p < 0.01$, ***$p < 0.001$, **** $p < 0.0001$

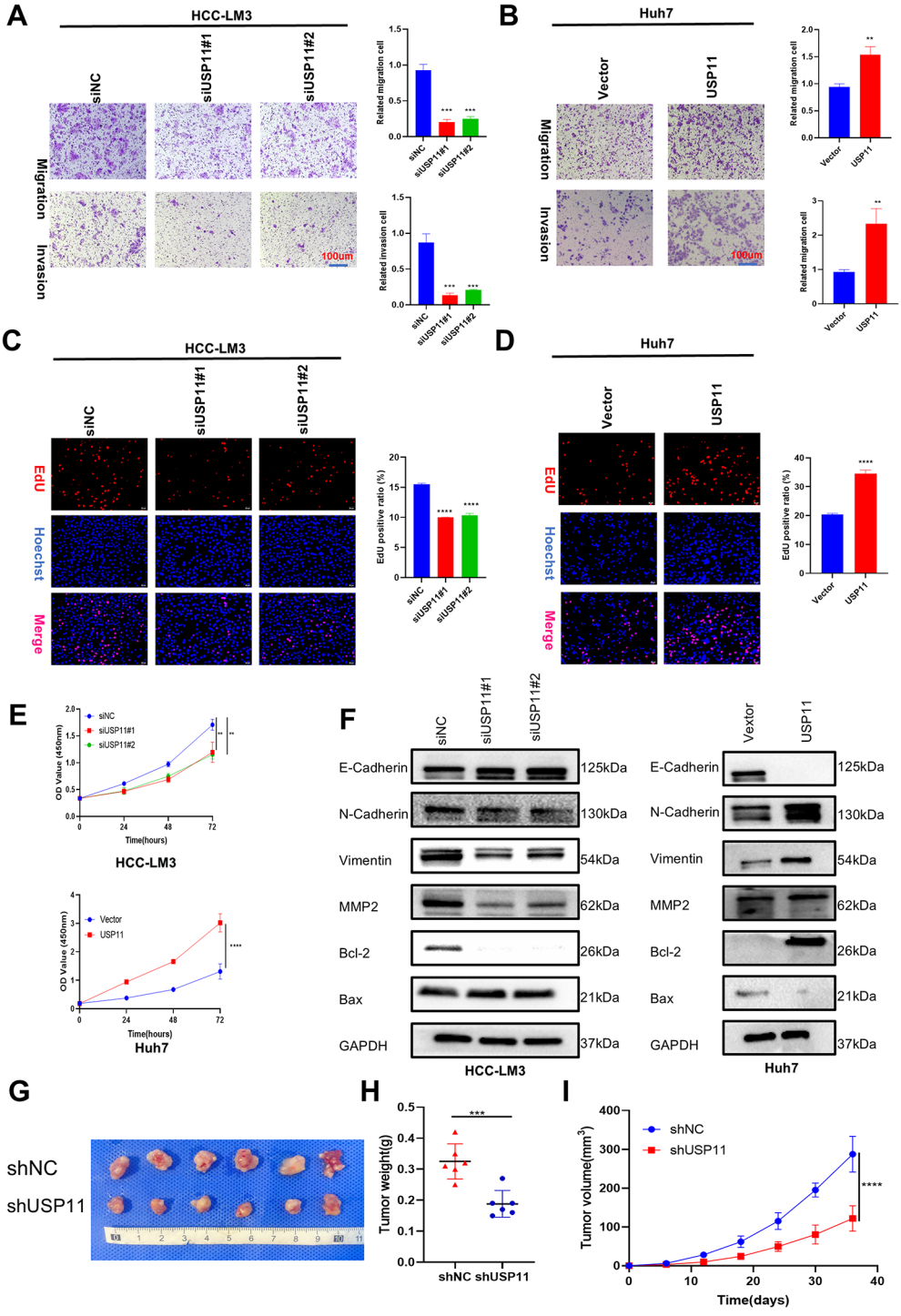

Fig. 5 USP11 deficiency attenuates the proliferation, migration and invasion of HCC cells. **A**. Representative images of Transwell assays in HCC-LM3 cells transfected with control siRNA or USP11 siRNA. Scale bar: 100 μm. **B**. Representative images of Transwell assays in Huh7 cells transfected with Vector or USP11. Scale bar: 100 μm. **C**. Representative images of EDU in HCC-LM3 cells transfected with control siRNA or USP11 siRNA. Scale bar: 20 μm. **D**. Representative images of EDU in Huh7 cells transfected with Vector or USP11. Scale bar: 20 μm. **E**.CCK-8 assays were used to assess the viability of HCC-LM3 and Huh7 cells. **F**. Expression of proteins associated with cell proliferation, apoptosis, migration, and invasion in HCC-LM3 and Huh7 cells. **G**. Overview of tumor formation in nude mice following subcutaneous injection of HCC-LM3 cells. **H**. Tumor size comparison between the shNC and shUSP11 groups. **I**. Measurement of tumor volume in both the shNC group and shUSP11 group at 6, 12, 18, 24,30 and 36 days. $^{**}p < 0.01$, $^{***}p < 0.001$, $^{****}p < 0.0001$

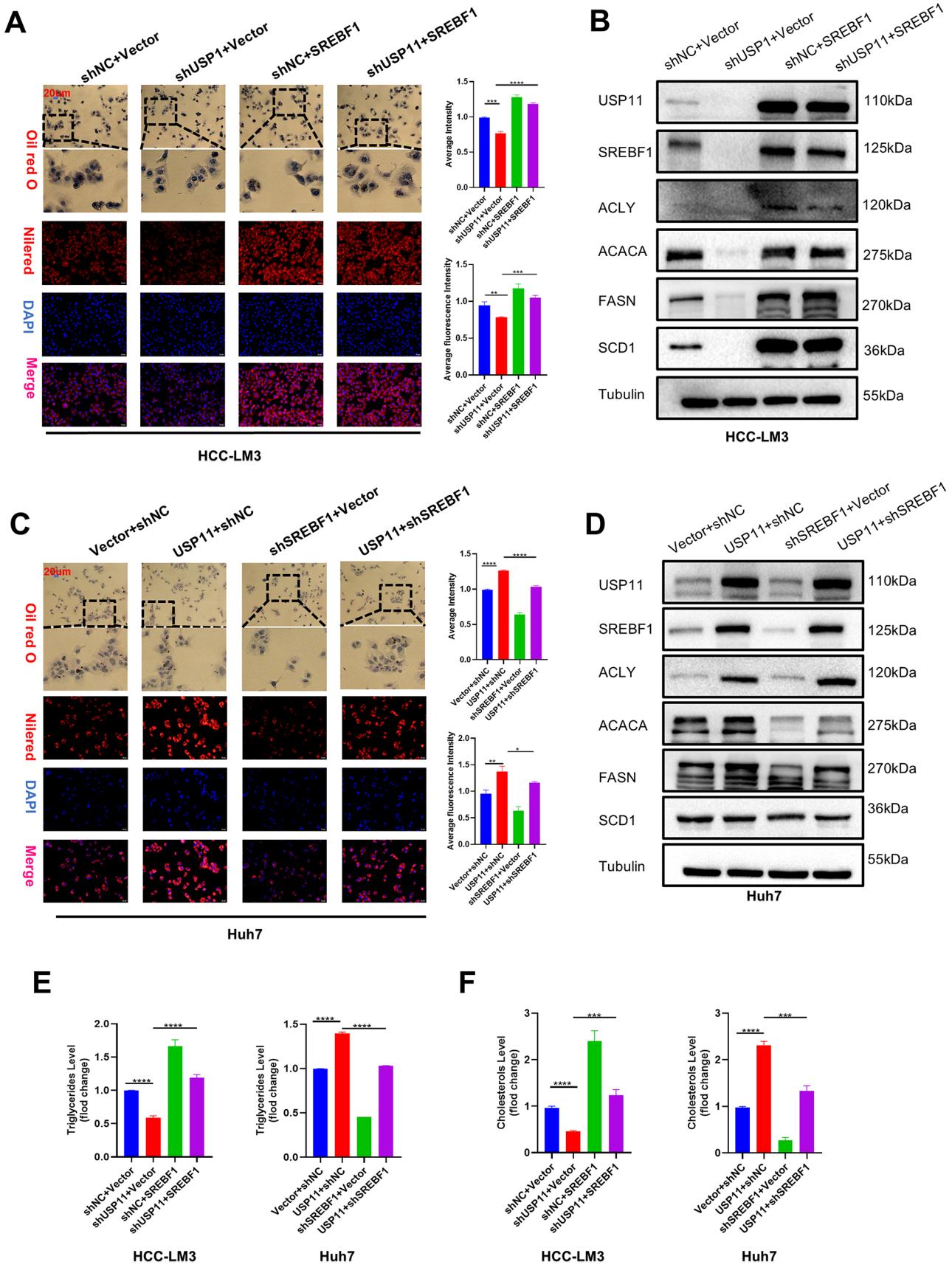

Fig. 6 (See legend on next page.)

(See figure on previous page.)

Fig. 6 USP11 accelerates HCC lipogenesis by up-regulating SREBF1. **A**. Oil red O staining (Upper) and Nile red staining (Lower) were used to evaluate the formation of lipids in HCC-LM3 cells. Scale bars, 20 μm. **B**. The levels of ACLY, ACACA, FASN and SCD1 were detected by western blotting in HCC-LM3 cells. **C**. Oil red O staining (Upper) and Nile red staining (Lower) were used to evaluate the formation of lipids in Huh7 cells. Scale bars, 20 μm. **D**. The levels of ACLY, ACACA, FASN and SCD1 were detected by western blotting in Huh7 cells. **E**. Triglycerides (Left panel) and cholesterol (Right panel) in HCC-LM3 cells were quantified using tissue-cell assay kits for triglycerides and total cholesterol. **F**. Triglycerides (Left panel) and cholesterol (Right panel) in Huh7 cells were quantified using tissue-cell assay kits for triglycerides and total cholesterol. *$p < 0.05$, **$p < 0.01$, ***$p < 0.001$, ****$p < 0.0001$

showed that silencing USP11 increased the apoptosis rate of HCC cells (Fig. S4A/C), while overexpressing USP11 inhibited these processes (Fig. S4B). Western blot analysis revealed that the expression levels of proteins related to cell proliferation, apoptosis, migration, and invasion were reduced in the experimental group compared to the control group, whereas overexpressing USP11 altered this phenomenon (Fig. 5F, Fig. S2G). In the subcutaneous tumor model, researchers observed that the tumor weight and volume in the USP11 knockdown group were smaller compared to the control group, further confirming the oncogenic role of USP11 in vivo (Fig. 5G-I).

USP11 accelerates HCC lipogenesis and progression by up-regulating SREBF1

Researchers conducted a complementation experiment to investigate whether the carcinogenic effect of USP11 depends on the stability of SREBF1 in HCC. Knocking down USP11 significantly reduces the lipogenesis, while these effects could also be reversed by upregulating SREBF1 expression in HCC-LM3(Fig. 6A/B/E/F) and HepG2 cells (Fig. S3A-C). Upregulating USP11 promoted the lipogenesis, while these effects could also be reversed by knocking SREBF1 expression in Huh7 cells (Fig. 6C-F). Additionally, inhibiting USP11 impeded migration, invasion, proliferation and colony formation in HCC-LM3(Fig. 7A-B) and HepG2 cells (Fig. S3D-E), while upregulating USP11 promoted these processes in Huh7 cells (Fig. 7C-D). Similarly, these effects could also be reversed by knocking down SREBF1 expression. In the apoptosis assays, overexpression of SREBF1 reduced the increased apoptosis caused by USP11 suppression (Fig. S4D-E), whereas the opposite effect was observed in Huh7 cells (Fig. S4F). Our research findings confirm that USP11 promotes tumor lipogenesis and progression by upregulating SREBF1.

The USP11/SREBF1 axis accelerates HCC lipid synthesis and growth in vivo

To assess the role of the USP11/SREBF1 axis in the malignant progression of HCC in vivo, HCC-LM3 cells transfected with lentiviruses carrying the corresponding genes were injected into nude mice to establish subcutaneous xenograft model (Fig. 8A). In the shUSP11 group, both the volume and weight of subcutaneous tumors were significantly reduced compared to the shNC group. Nevertheless, the reintroduction of SREBF1 substantially promoted tumor growth in HCC-LM3 cells, even without USP11 (Fig. 8B-C).Knockdown of USP11 disrupted lipid synthesis in subcutaneous tumors, but overexpression of SREBF1 reversed this effect, as evidenced by measurements of triglycerides and cholesterol in the tumor tissues (Fig. 8D).Moreover, immunohistochemical analysis showed that USP11 suppression resulted in lower levels of the proliferation marker Ki67 and reduced Oil Red O staining in subcutaneous tumors. Conversely, the overexpression of SREBF1 reversed these effects (Fig. 8E). Additionally, the elevated expression of SREBF1 significantly reversed the reduction in lung metastasis triggered by USP11 knockdown (Fig. 8E). In summary, these findings suggest that USP11 modulates lipid synthesis, growth, and metastasis in HCC cells via SREBF1.

Elevated USP11 expression is correlated with increased SREBF1 levels and serves as an indicator of poor prognosis in HCC patients

To evaluate the clinical relevance of USP11 and SREBF1 in HCC patients, we analyzed the expression of USP11 and SREBF1 in 78 HCC samples. The results showed that, compared to normal liver tissue, the mRNA levels of USP11 and SREBF1 were significantly elevated in HCC tissue (Fig. 9A-B). Similarly, the expression of USP11 and SREBF1 proteins was also upregulated in HCC tissue (Fig. 9C-F). Additionally, the protein levels of USP11 positively correlated with those of SREBF1, which was verified by the Pearson correlation analysis (Fig. 9G). Importantly, patients with higher levels of USP11 or SREBF1 protein had lower overall survival rates compared to those with lower protein levels (Fig. 9H-I). Notably, these clinical data support our preclinical discovery that USP11 regulates the deubiquitination and stabilization of SREBF1, thereby driving the progression of HCC.

Discussion

Hepatocellular carcinoma (HCC) remains a major challenge due to its high incidence and poor prognosis [1]. Late-stage diagnosis hampers the effectiveness of existing treatments, such as sorafenib and lenvatinib [22, 23]. To improve therapeutic strategies, a deeper understanding of the molecular mechanisms driving HCC is essential. In recent years, the role of dysregulated lipid metabolism in the occurrence and development of HCC has garnered significant attention [24–26]. Exploring the connection between HCC and lipid metabolism

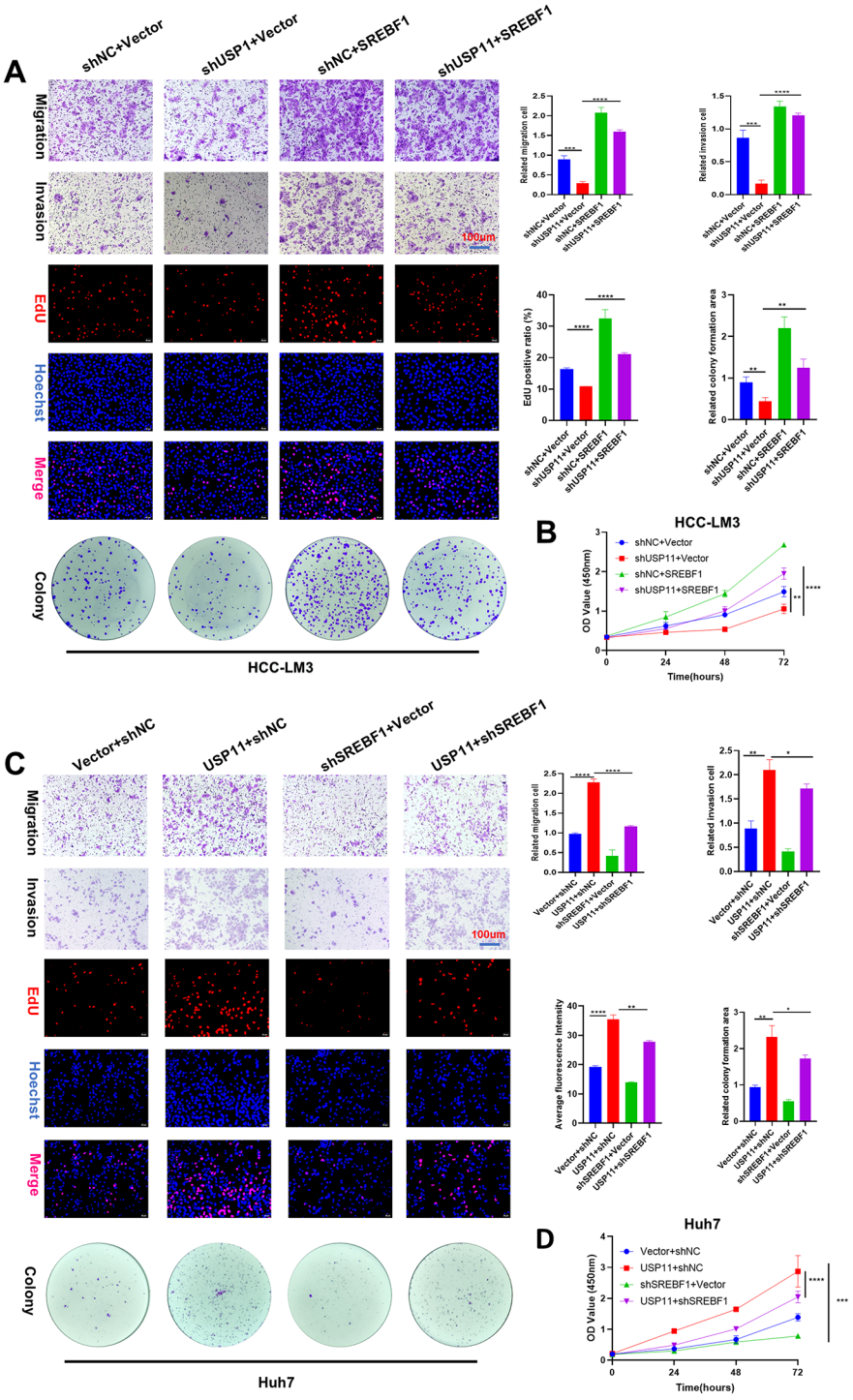

Fig. 7 USP11 accelerates HCC progression by up-regulating SREBF1. **A**. Representative images of Transwell assay (Upper), EDU(Middle) and colony formation (Lower) in HCC-LM3 cells. Scale bar: 100 μm; 20 μm. **B**.CCK-8 assays were utilized to measure the viability of HCC-LM3 cells. **C**. Representative images of Transwell assays (Upper), EDU(Middle) and colony formation (Lower) in Huh7 cells. Scale bar: 100 μm; 20 μm. **D**.CCK-8 assays were utilized to measure the viability of Huh7 cells. *$p < 0.05$, **$p < 0.01$, ***$p < 0.001$, ****$p < 0.0001$

has revealed it as a promising new target for developing anti-HCC medications [27, 28].Our study reveals that USP11 is a critical oncoprotein in HCC, crucial for tumor progression by stabilizing SREBF1, a key transcription factor involved in lipogenesis. Significantly, the truncated mutant USP11 (503–938 aa) interacts with the truncated mutant SREBF1 (569–1147 aa), with K1151 playing a crucial role in this interaction. This interaction supports

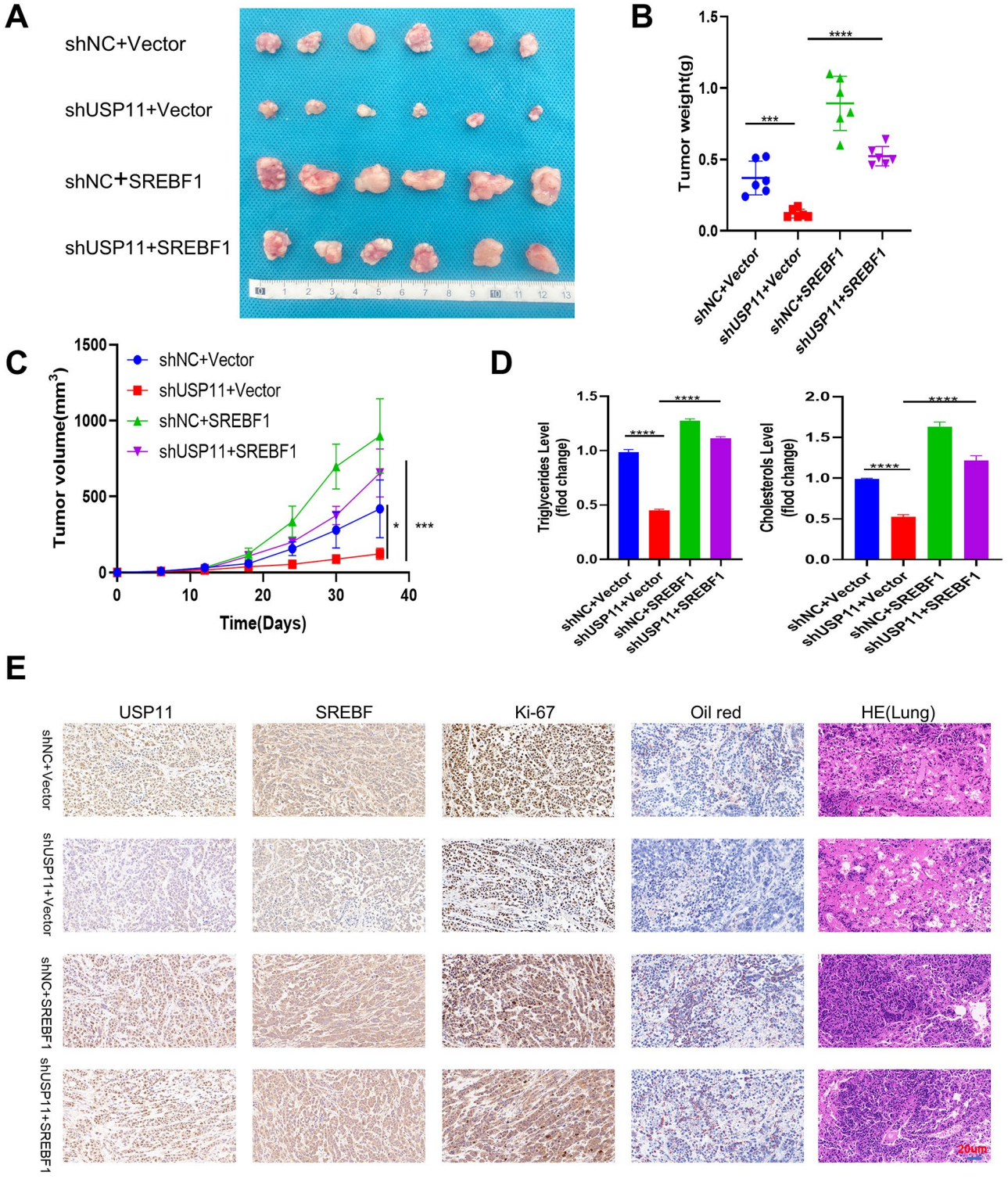

Fig. 8 The USP11/SREBF1 axis regulates HCC cell lipogenesis and tumorigenesis in vivo. **A**. Images of resected subcutaneous tumors from the HCC-LM3 cell in nude mice. **B**. Tumor weight **C**. Tumor size **D**. The levels of triglycerides and cholesterol in subcutaneous tumors, respectively. **E**. Expression of USP11, SREBF1, Ki67 and Oil Red O in subcutaneous tumors, and representative images of H&E staning of lung. Scale bars: 20 μm. * $p < 0.05$; *** $p < 0.001$; **** $p < 0.0001$

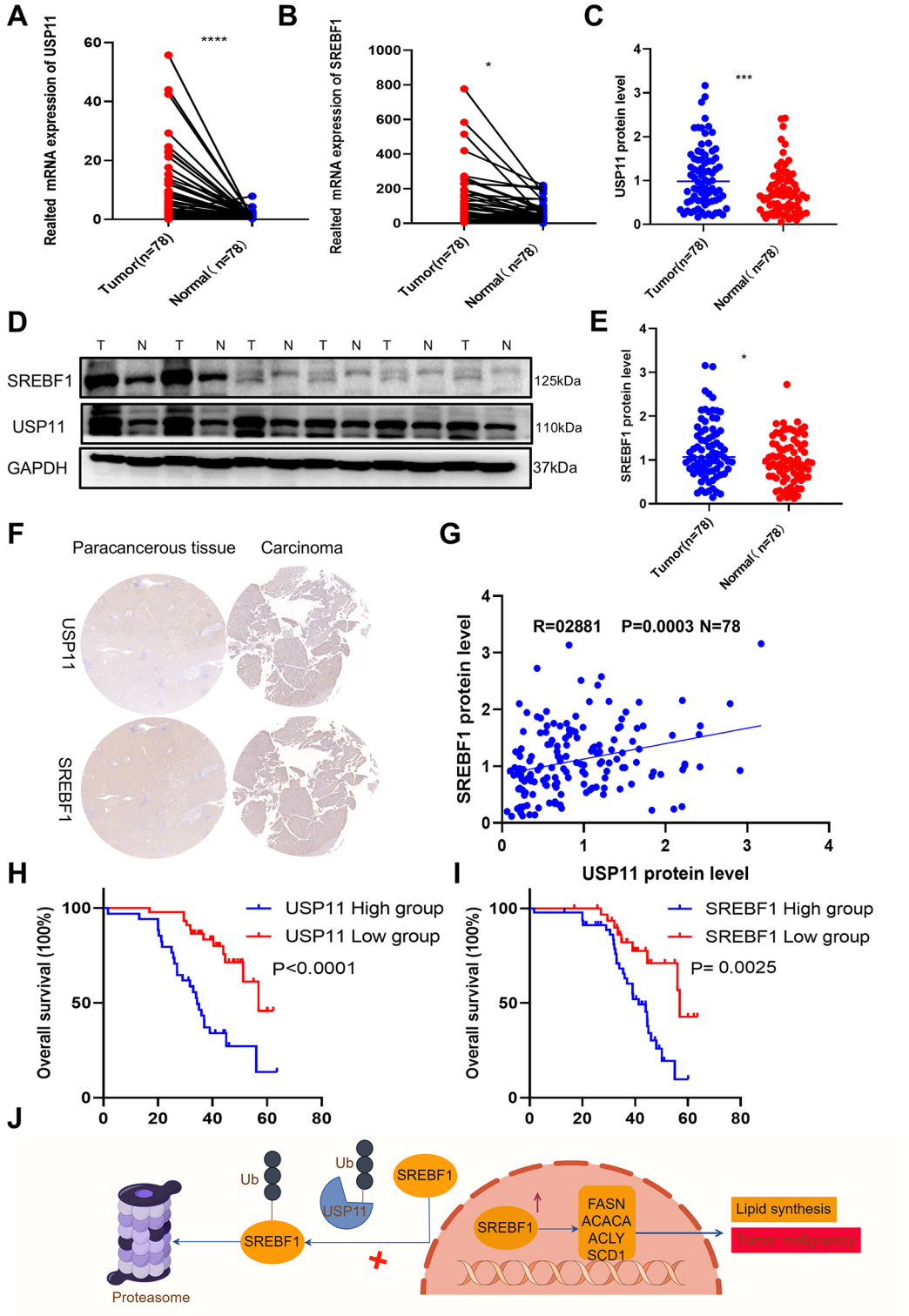

Fig. 9 USP11 is positively correlated with SREBF1 in HCC patients. **A**. Assessment of mRNA expression levels of USP11 in paired HCC and adjacent non-tumor tissues. **B**. Assessment of mRNA expression levels of SREBF1 in paired HCC and adjacent non-tumor tissues. **C**. Quantification of USP11 protein expression in tissues. **D**. The expression of USP11 and SREBF1 at the protein level in HCC compared to normal tissues. **E**. Quantification of SREBF1 protein expression in tissues. **F**. Immunohistochemical assay performed on HCC and adjacent normal tissue microarrays ($n = 78$), showing representative images of USP11 and SREBF1. **G.** The correlation between USP11 and SREBF1 protein levels in HCC. **H**. Kaplan-Meier survival curves for HCC patients with low and high USP11expression. **I**. Kaplan-Meier survival curves for HCC patients with low and high SREBF1 expression. **J**. Graphical summary of USP11-regulated lipid synthesis and proliferation in HCC. * $p < 0.05$; *** $p < 0.001$; **** $p < 0.0001$

the stability of SREBF1, thereby promoting the transcription of key enzymes in lipid metabolism processes such as ACLY, FASN, ACACA, and SCD1, and facilitating lipid synthesis and tumorigenesis in HCC. Moreover, the alterations in mRNA and Western blot levels of key lipid metabolism enzymes such as ACLY, FASN, ACACA, and SCD1, which are influenced by USP11, depend on the involvement of SREBF1.In addition, we demonstrated clinical evidence of upregulation and positive correlation between USP11 and SREBF1 in HCC samples. The discovery of the USP11-SREBF1 axis presents promising therapeutic targets for HCC, potentially broadening the development of new DUB inhibitors and introducing cancer treatment strategies focused on lipid-related pathways.

SREBF1, a key regulator of lipid metabolism, has recently been implicated in cancer development [29]. In eukaryotic cells, SREBF1 influences various cellular processes beyond lipid biosynthesis, including cell growth, migration, and drug resistance [4, 30]. SREBF1 is upregulated in colorectal cancer, enhancing cell invasion and metastasis by mediating MMP7 expression and activating the NF-κB pathway [31]. It also boosts ROS-induced killing of melanoma cells and inhibits BRAF-mediated drug resistance [32].In this study, we identified SREBF1 as a potential binding protein of USP11 through immunoprecipitation and mass spectrometry analysis. We further demonstrated that USP11 directly binds to and stabilizes SREBF1. The decrease in SREBF1 protein levels due to USP11 deficiency was significantly prevented by the proteasome inhibitor MG132, indicating that SREBF1 degradation is regulated by the ubiquitin-proteasome pathway. The deubiquitination activity of USP11 results in elevated SREBF1 protein levels, promoting the transcription of lipid synthesis-related target genes, such as ACLY, ACACA, FASN, and SCD1. Consistent with our findings, recent studies have reported that DDX39B and TRIM21 also contribute to in tumor lipid metabolism by regulating SREBF1 [17, 29]. Additionally, we observed that USP11 deficiency in knockdown HCC cells downregulates key lipid metabolism enzymes controlled by SREBF1. Similarly, DDX39B enhances lipid synthesis and malignant progression in HCC by augmenting the transcription factor function of nuclear SREBF1 [29]. Furthermore, USP11 has been shown to interact with HIF-1α, promoting the expression of glycolysis-related genes and cell proliferation in HCC [33]. These studies further support the critical role of USP11 in regulating the interplay between glucose and lipid metabolism in cancer cells. Therefore, developing small molecule inhibitors targeting USP11 could offer an effective therapeutic strategy for HCC.

In recent years, DUBs have been extensively studied for their potential role in stabilizing oncoproteins. USP11 is one of the largest members of cysteine protease DUB family members and is involved in regulating cell cycle, DNA repair, signal transduction, tumor development, and other important biological processes [34]. Zhang et al. found that USP11 functions as a tumor suppressor in kidney cancer by deubiquitinating and stabilizing VGLL4 protein [35]. Wang et al. reported that the interaction between HK2 and CD133 promotes the binding of USP11 to CD133, inhibiting its polyubiquitination and degradation, thereby facilitating tumor immune evasion and cancer stemness [36]. However, the role of USP11 in HCC remains to be clarified. There are currently few studies reporting how USP11 binds to downstream target proteins through specific binding sites to exert its function. By dividing the USP11 sequence into four peptide segments (M1: 1-938aa, M2: 1-284aa, M3: 503–963aa, and M4: 285–963aa), we found that only M2 does not bind to SREBF1. Additionally, K1151 was identified as a key ubiquitination site of USP11 in regulating the ubiquitination level of SREBF1.

Increasing evidence suggests that lipid metabolism is involved in tumorigenesis and is associated with the prognosis of cancer patients. Identifying key proteins or regulatory genes in the complex pathways of lipid metabolism and targeting pathways that promote tumor cell proliferation may provide new therapeutic targets for cancer [37]. Our study found that the loss of the USP11-SREBF1 axis significantly reduced lipid synthesis and malignant proliferation in HCC cells. As a transcription factor, SREBF1 activates metabolic reprogramming by regulating multiple downstream genes such as ACLY, ACACA, FASN, and SCD1 [38]. Our data indicate that upregulation of the USP11-SREBF1 axis is associated with reduced overall survival and relapse-free survival in HCC patients. However, there are several limitations to our study. On one hand, only a single animal model was established to assess the in vivo role of the USP11-SREBF1 axis. On the other hand, further research is needed to explore how SREBF1 regulates the expression of downstream metabolic enzymes ACLY, ACACA, FASN, and SCD1 as a transcription factor. Additionally, there is an urgent need to develop effective inhibitors targeting the USP11-SREBF1 axis and evaluate their impact on HCC proliferation and metastasis in preclinical and clinical studies.

In conclusion, our study highlights that USP11 enhances lipogenesis and tumorigenesis in HCC by regulating SREBF1 stability. Targeting the USP11-SREBF1 axis represents a promising approach for novel therapeutic interventions in advanced HCC.

Supplementary Information

The online version contains supplementary material available at https://doi.org/10.1186/s12964-024-01926-x.

Supplementary Material 1: Supplementary Data 1

Supplementary Material 2: Supplemental Data 2

Acknowledgements
This research was supported by a funding from National Natural Science Foundation of China (No.82460609, No.82060435, No.82160602), Jiangxi Provincial Natural Science Foundation(20204BCJ22027), 2024 Changyi Leading Research (ZL049) and the Beijing science and technology innovation medical development foundation (KC2023-JX-0288-FZ127).We acknowledged the use of Figuredraw (https://www.Figuredraw.com) to create the follow diagram.

Author contributions
XYK, HSL, MY, WJB conceived the study and designed the experiments. XYK, ZJY, LK, FSM performed the experiments, collected the data. MY, TS, LD, HSL, WJB provided technical and and material support. XYK, HSL and WJB provided material support and revised the manuscript. All authors read and approved the final manuscript.

Data availability
No datasets were generated or analysed during the current study.

Declarations

Ethics approval and consent to participate
The Ethics Committee of the Second Affiliated Hospital of Nanchang University approved the inclusion of human participants and the use of human data and tissues in this study, and conducted them in accordance with the principles of the Declaration of Helsinki. All animal experiments were approved by the Institutional Animal Care and Use Committee of Nanchang Royo Biotech Co., Ltd. (Ethics ID: RYE2023120301)

Competing interests
The authors declare no competing interests.

Received: 18 September 2024 / Accepted: 4 November 2024
Published online: 18 November 2024

References

1. Vogel A, Meyer T, Sapisochin G et al. Hepatocellular carcinoma[J] Lancet 2022,400(10360):1345–62.
2. Zhao Y, Li ZX, Zhu YJ et al. Single-cell transcriptome analysis uncovers Intratumoral Heterogeneity and underlying mechanisms for Drug Resistance in Hepatobiliary Tumor Organoids[J]. Adv Sci (Weinh) 2021,8(11):e2003897.
3. Du D, Liu C, Qin M, et al. Metabolic dysregulation and emerging therapeutical targets for hepatocellular carcinoma[J]. Acta Pharm Sin B. 2022;12(2):558–80.
4. Shimano H, Sato R. SREBP-regulated lipid metabolism: convergent physiology - divergent pathophysiology[J]. Nat Rev Endocrinol 2017,13(12):710–30.
5. Chen M, Li H, Zheng S et al. Nobiletin targets SREBP1/ACLY to induce autophagy-dependent cell death of gastric cancer cells through PI3K/Akt/mTOR signaling pathway[J]. Phytomedicine,2024,128:155360.
6. Han LQ, Gao TY, Yang GY et al. Overexpression of SREBF chaperone (SCAP) enhances nuclear SREBP1 translocation to upregulate fatty acid synthase (FASN) gene expression in bovine mammary epithelial cells[J]. J Dairy Sci 2018,101(7):6523–31.
7. Wang X, Sun Z, Gao Y, et al. 3-tert-butyl-4-hydroxyanisole perturbs renal lipid metabolism in vitro by targeting androgen receptor-regulated de novo lipogenesis[J]. Ecotoxicol Environ Saf. 2023;258:114979.
8. Chen H, Qi Q, Wu N, et al. Aspirin promotes RSL3-induced ferroptosis by suppressing mTOR/SREBP-1/SCD1-mediated lipogenesis in PIK3CA-mutant colorectal cancer[J]. Redox Biol. 2022;55:102426.
9. Chen J, Ding C, Chen Y, et al. ACSL4 reprograms fatty acid metabolism in hepatocellular carcinoma via c-Myc/SREBP1 pathway[J]. Cancer Lett. 2021;502:154–65.
10. Chen J, Wu Z, Ding W et al. SREBP1 siRNA enhance the docetaxel effect based on a bone-cancer dual-targeting biomimetic nanosystem against bone metastatic castration-resistant prostate cancer[J]. Theranostics 2020,10(4):1619–32.
11. Ma X, Zhao T, Yan H, et al. Fatostatin reverses progesterone resistance by inhibiting the SREBP1-NF-kappaB pathway in endometrial carcinoma[J]. Cell Death Dis. 2021;12(6):544.
12. Liu C, Chikina M, Deshpande R et al. Treg cells promote the SREBP1-Dependent metabolic fitness of Tumor-promoting macrophages via repression of CD8(+) T cell-derived Interferon-gamma[J]. Immunity,2019,51(2):381–97.
13. Gu X, Nardone C, Kamitaki N et al. The midnolin-proteasome pathway catches proteins for ubiquitination-independent degradation[J]. Sci 2023,381(6660):h5021.
14. Ernst A, Avvakumov G, Tong J et al. A strategy for modulation of enzymes in the ubiquitin system[J]. Sci 2013,339(6119):590–5.
15. Sun T, Liu Z, Yang Q. The role of ubiquitination and deubiquitination in cancer metabolism[J]. Mol Cancer. 2020;19(1):146.
16. Popovic D, Vucic D, Dikic I. Ubiquitination in disease pathogenesis and treatment[J]. Nat Med 2014,20(11):1242–53.
17. Chen X, Yong H, Chen M, et al. TRIM21 attenuates renal carcinoma lipogenesis and malignancy by regulating SREBF1 protein stability[J]. J Exp Clin Cancer Res. 2023;42(1):34.
18. Dewson G, Eichhorn P, Komander D. Deubiquitinases in cancer[J]. Nat Rev Cancer 2023,23(12):842–62.
19. Komander D, Clague MJ, Urbe S. Breaking the chains: structure and function of the deubiquitinases[J]. Nat Rev Mol Cell Biol. 2009;10(8):550–63.
20. Lange SM, Armstrong LA, Kulathu Y, Deubiquitinases. From mechanisms to their inhibition by small molecules[J]. Mol Cell. 2022;82(1):15–29.
21. Ning Z, Guo X, Liu X, et al. USP22 regulates lipidome accumulation by stabilizing PPARgamma in hepatocellular carcinoma[J]. Nat Commun. 2022;13(1):2187.
22. Llovet JM, Ricci S, Mazzaferro V, et al. Sorafenib in advanced hepatocellular carcinoma[J]. N Engl J Med. 2008;359(4):378–90.
23. Kudo M, Finn RS, Qin S et al. Lenvatinib versus Sorafenib in first-line treatment of patients with unresectable hepatocellular carcinoma: a randomised phase 3 non-inferiority trial[J]. Lancet 2018,391(10126):1163–73.
24. Bian X, Liu R, Meng Y et al. Lipid metabolism and cancer[J]. J Exp Med,2021,218(1).
25. Martin-Perez M, Urdiroz-Urricelqui U, Bigas C, et al. The role of lipids in cancer progression and metastasis[J]. Cell Metab. 2022;34(11):1675–99.
26. Phan LM, Yeung SC, Lee MH. Cancer metabolic reprogramming: importance, main features, and potentials for precise targeted anti-cancer therapies[J]. Cancer Biol Med. 2014;11(1):1–19.
27. Cao LQ, Xie Y, Fleishman JS, et al. Hepatocellular carcinoma and lipid metabolism: novel targets and therapeutic strategies[J]. Cancer Lett. 2024;597:217061.
28. Terry AR, Hay N. Emerging targets in lipid metabolism for cancer therapy[J]. Trends Pharmacol Sci 2024,45(6):537–51.
29. Feng T, Li S, Zhao G et al. DDX39B facilitates the malignant progression of hepatocellular carcinoma via activation of SREBP1-mediated de novo lipid synthesis[J]. Cell Oncol (Dordr) 2023,46(5):1235–52.
30. Zhao Q, Lin X, Wang G. Targeting SREBP-1-Mediated lipogenesis as potential strategies for Cancer[J]. Front Oncol. 2022;12:952371.
31. Gao Y, Nan X, Shi X, et al. SREBP1 promotes the invasion of colorectal cancer accompanied upregulation of MMP7 expression and NF-kappaB pathway activation[J]. BMC Cancer. 2019;19(1):685.
32. Wu S, Naar AM. SREBP1-dependent de novo fatty acid synthesis gene expression is elevated in malignant melanoma and represents a cellular survival trait[J]. Sci Rep. 2019;9(1):10369.
33. Qiao L, Hu W, Li L et al. USP11 promotes glycolysis by regulating HIF-1alpha stability in hepatocellular carcinoma[J]. J Cell Mol Med 2024,28(2):e18017.
34. Liao Y, Zhou D, Wang P, et al. Ubiquitin specific peptidase 11 as a novel therapeutic target for cancer management[J]. Cell Death Discov. 2022;8(1):292.
35. Zhang E, Shen B, Mu X et al. Ubiquitin-specific protease 11 (USP11) functions as a tumor suppressor through deubiquitinating and stabilizing VGLL4 protein[J]. Am J Cancer Res 2016,6(12):2901–9.
36. Wang J, Shao F, Yang Y et al. A non-metabolic function of hexokinase 2 in small cell lung cancer: promotes cancer cell stemness by increasing USP11-mediated CD133 stability[J]. Cancer Commun (Lond) 2022,42(10):1008–27.

37. Wang R, Hu Q, Wu Y et al. Intratumoral lipid metabolic reprogramming as a pro-tumoral regulator in the tumor milieu[J]. Biochim Biophys Acta Rev Cancer 2023,1878(5):188962.
38. Zhou Y, Tao J, Calvisi DF et al. Role of Lipogenesis Rewiring in Hepatocellular Carcinoma[J]. Semin Liver Dis 2022,42(1):77–86.

Publisher's note